

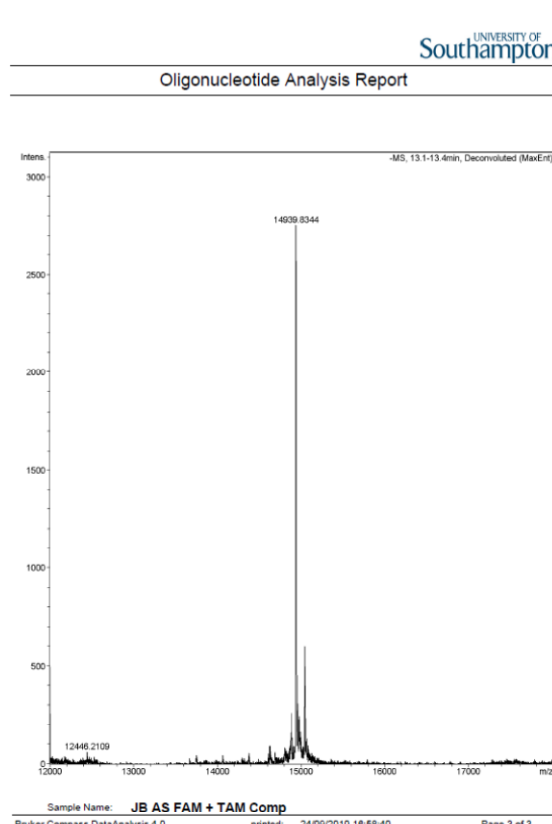
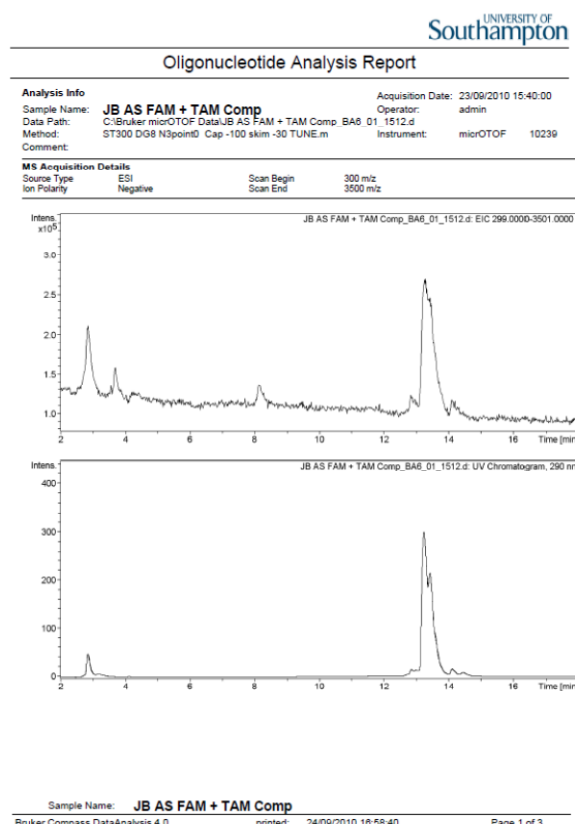
Electronic Supporting Information

A DNA based five-state switch with programmed reversibility

Jonathan R. Burns,^a Søren Preus,^b Daniel G. Singleton^a and Eugen Stulz*^a

General

Solid supported DNA synthesis reagents were purchased from SAFC Proligo, DNA purification columns were purchased from Glen Research and Berry and Associates, desalting columns were purchased from GE Healthcare. DNA Melting profiles were recorded using a Varian Cary 300 Spectrophotometer and on a Varian Eclipse fluorescence spectrometer in quartz cells with path length of 1 cm are an average of at least two denaturing-annealing cycles. The absorptions of oligonucleotide solutions were measured at 260 nm in a quartz cuvette with a path length of 1 cm. The unmodified DNA strands and the FAM/TAMRA labelled DNA was obtained from ATDBio Ltd (Southampton, UK); the FAM/TAMRA-DNA was confirmed using ESI MS (negative mode) on Bruker micrOTOF.



²⁰ m/z calcd 14940.47 Da; found 14939.83 ($M-H^-$).

Porphyrin DNA synthesis

Rigid and flexible porphyrin monomers were prepared according to published protocols.^[1, 2] To generate a singularly modified zinc porphyrin on the DNA, the final acid deprotection step during solid phase DNA synthesis was omitted, after which the labelled DNA was deprotected and purified using PolyPack affinity columns by the same protocols as published previously. Porphyrin labelled DNA was purified by RP-HPLC.

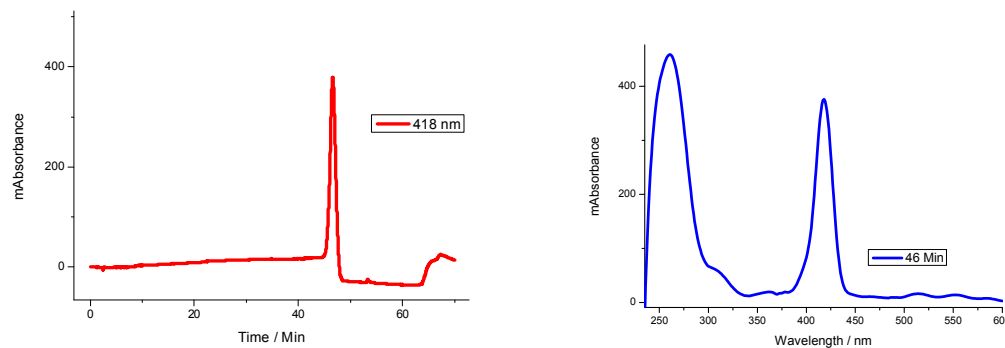


Figure S1. HPLC chromatogram of 1P, using a HFIP/MeOH gradient as described by Berova *et. al.*^[3] using a Waters Xbridge OST C18 2.5 μ M 4.6 x 50 mm column (left) and UV-Vis absorption cross-section at 46 minutes (right).

DNA analysis

Release DNA sequences (complementary strands to **2 – 6**):

15	2a	ATTA TAAT ATTA TAAT ATTA TAAT ATTA CGA CAT TGA TTT CTC ACA CTC-5'
	3a	ATTA TAAT ATTA TAAT ATTA TAAT CGA CAT TGA TTT CTC ACA CTC-5'
	4a	ATTA TAAT ATTA TAAT CGA CAT TGA TTT CTC ACA CTC-5'
20	5a	ATTA TAAT CGA CAT TGA TTT CTC ACA CTC-5'
	6a	CGA CAT TGA TTT CTC ACA CTC-5'

DNA was annealed using the peltier device on a Varian Cary 300 Biospectrophotometer or Varian Eclipse Spectrometer. DNA was annealed at 1 °C / min. Concentrations determined using ϵ at 260 nm as shown in Table S1.

25 Table S1:

Strand	Sequence	ϵ_{260}
1	<u>A</u> AAT ATTA TAAT ATTA TAAT ATTA G <u>C</u> T GTA ACT AAA G 3'	481800
	ATTA TAAT ATTA TAAT ATTA TAAT ATTA CGA CAT TGA TTT CTC ACA	538100
2	CTC-5'	
3	ATTA TAAT ATTA TAAT ATTA CGA CAT TGA TTT CTC ACA CTC-5'	451700
4	ATTA TAAT ATTA TAAT CGA CAT TGA TTT CTC ACA CTC-5'	365300
5	ATTA TAAT CGA CAT TGA TTT CTC ACA CTC-5'	278900
6	CGA CAT TGA TTT CTC ACA CTC-5'	191700
2a	TAAT ATTA TAAT ATTA TAAT ATTA GCT GTA ACT AAA GAG TGA GAG 3'	566500
3a	TAAT ATTA TAAT ATTA TAAT GCT GTA ACT AAA GAG TGA GAG 3'	480100
4a	TAAT ATTA TAAT ATTA GCT GTA ACT AAA GAG TGA GAG 3'	393700
5a	TAAT ATTA GCT GTA ACT AAA GAG TGA GAG 3'	307300
6a	GCT GTA ACT AAA GAG TGA GAG 3'	221500
D	AAAT ATTA TAAT ATTA TAAT ATTA G <u>C</u> T GTA ACT AAA G 3'	481800

Quantum yield and overlap integral determination of the FAM and TAMRA FRET pair

The quantum yield of FAM in DNA was determined using monomeric FAM in aqueous solution as reference ($QY = 0.95$) at an excitation wavelength of 495 nm. The overlap integral between the FAM emission spectrum and TAMRA absorption spectrum was calculated to be $3.1 \times 10^5 \text{ M}^{-1} \text{ cm}^{-1} \text{ nm}^4$ yielding a critical Förster distance of $R_0 = 57 \text{ Å}$. The UV-Vis absorption and emission spectra are shown in Figure S2.

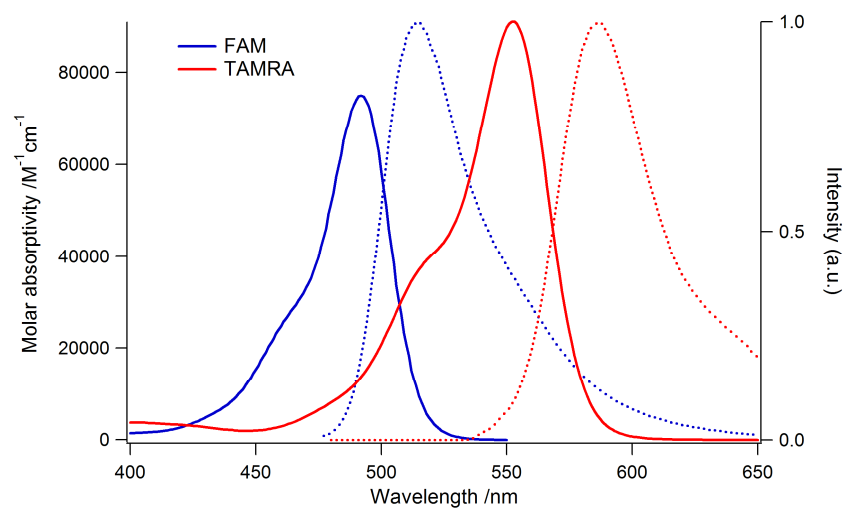


Figure S2. Molar extinction coefficient spectra of FAM and TAMRA and their normalized emission spectra.

Quantum yield and overlap integral determination of Zn- and 2H-porphyrin DNA

The quantum yield and overlap integral value for zinc- and 2H-porphyrin DNA was determined using a control 21-mer DNA sequence shown below. The UV-Vis absorption and fluorescence spectra are shown in Figure S3 and S4 respectively. The overlap between donor emission spectrum and acceptor absorption spectrum is shown in Figure S5.

$Z^1 = \text{Zn-porphyrin DNA} = 3' \text{ T ATT CAT ACA ACA } \underline{\text{1TG ATT TC}} 5'$

where 1 = Zn-porphyrin modification

$H^1 = \text{2H-porphyrin DNA} = 5' \text{ A TAA GTA TGT TGT AAC } \underline{\text{1AA AG}} 3'$

where 1 = 2H-porphyrin modification

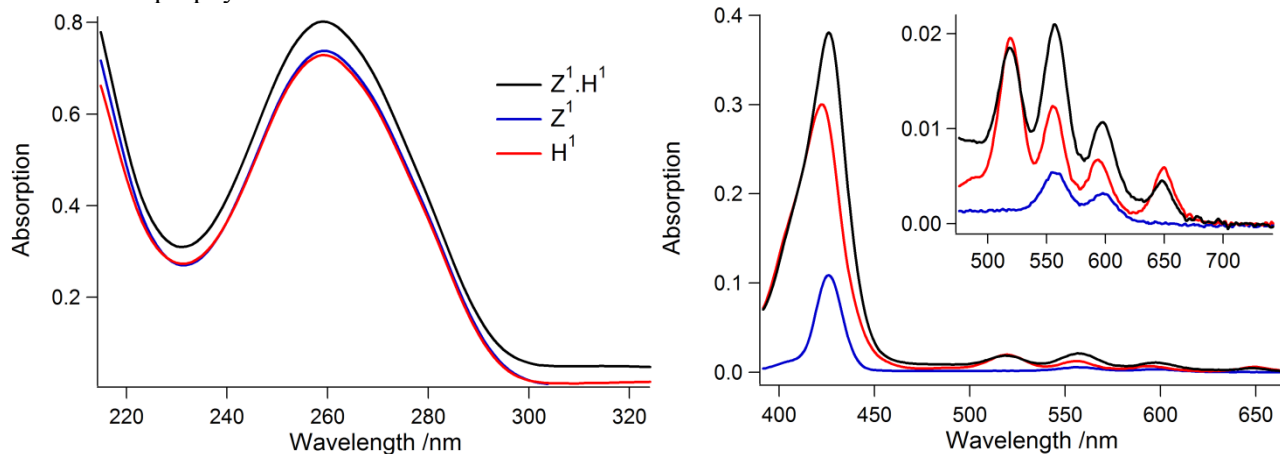


Figure S3. UV-Vis absorption spectra of DNA region (left) and porphyrin Soret band region (right) and Q-band region expanded (inset), at 2 μM in 0.1 M sodium phosphate buffer using a 1 cm path length cell.

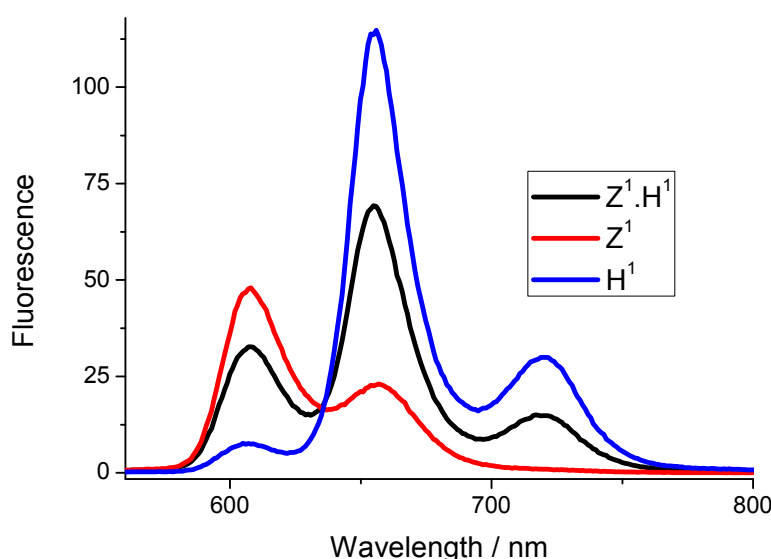


Figure S4. Fluorescence emission of Zn-porphyrin duplex DNA (Z^1 red line), 2H-porphyrin duplex DNA (H^1 blue line) and zinc and 2H porphyrin duplex DNA ($Z^1 \cdot H^1$ black line), excitation at 424 nm, at 2 μ M in 0.1 M sodium phosphate buffer, 1 cm quartz cell, scanning at 600 nm per minute, 500 PMT voltage.

5

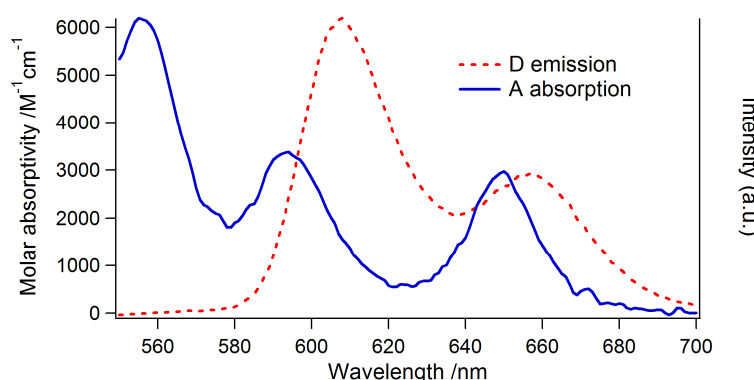


Figure S5. Overlayed Zn-porphyrin (D) emission spectrum and free base porphyrin (A) absorption spectrum.

10

Zn/H-porphyrin DNA switch UV-Vis and Fluorescence analysis

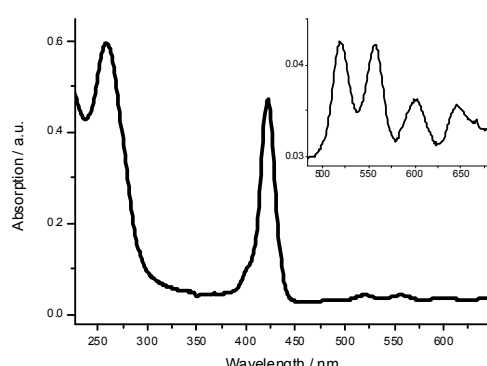


Figure S6. **1P** UV-Vis absorption spectra of DNA region and porphyrin Soret band region, and Q-band region expanded (inset), at 1 μ M in 0.1 M sodium phosphate buffer using a 1 cm path length cell.

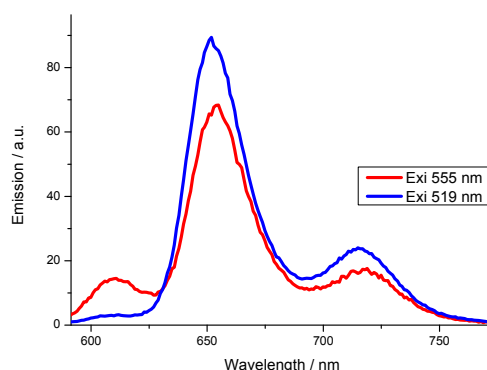


Figure S7. Fluorescence emission of **1P**, excitation at 555 nm (donor excitation, red line), and excitation at 519 nm (acceptor emission, blue line), at 2 μ M in 0.1 M sodium phosphate buffer, 1 cm quartz cell, scanning at 600 nm per minute, 600 PMT voltage.

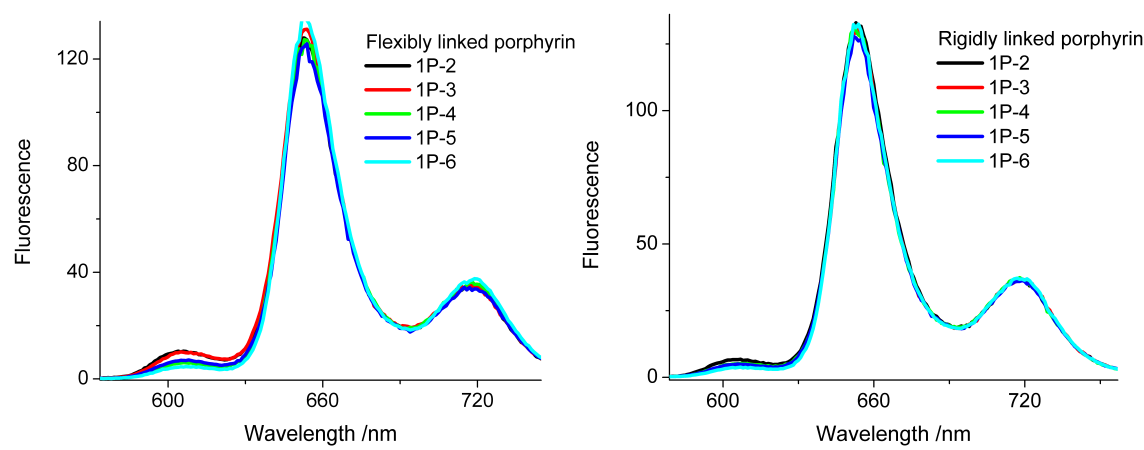


Figure S8. Emission spectra of donor+acceptor porphyrins in the DNA switch tethered via flexible (left) or rigid linkers (right) using an excitation wavelength of 426 nm. Calculated FRET efficiencies are plotted in Figure S13.

1F variable annealing rate UV analysis

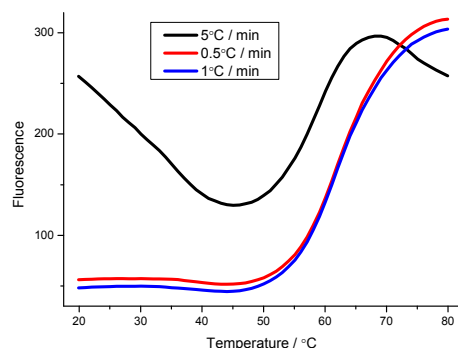


Figure S9. Fluorescence annealing profile monitoring **1F** donor emission, at 0.3 μ M in 0.1 M sodium phosphate buffer, excitation at 495 nm, emission at 510 nm, annealing at 5 °C / min (black line), 1 °C / min (blue line) and 0.5 °C / min (red line), using a 1 cm quartz cell, 500 PMT voltage.

1P DNA region UV melting analysis

10

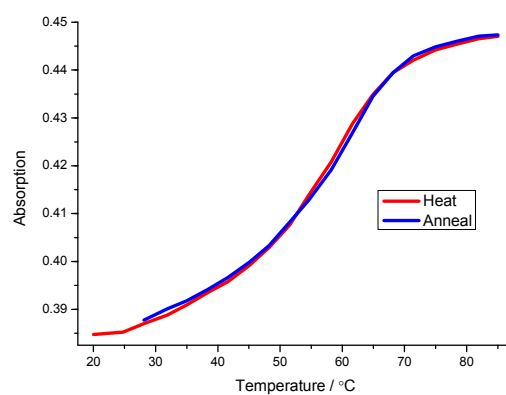


Figure S10. UV melting profile of **1P** recorded at 422 nm, at 1 μ M in 0.1 M sodium phosphate buffer, heating and annealing at 1 °C / min, 1 cm quartz cell.

1F Fluorescence melting analysis - acceptor emission

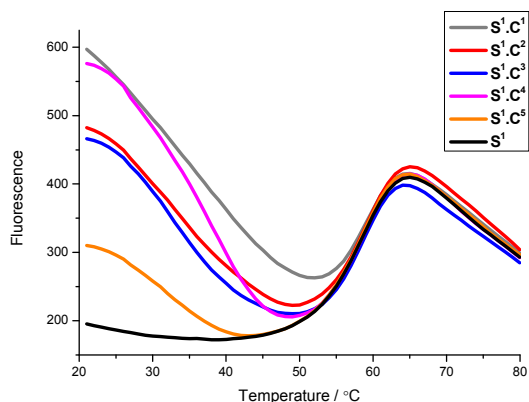


Figure S11. Fluorescence melting profile of **1F** acceptor emission combinations, at 0.3 μ M in 0.1 M sodium phosphate buffer, excitation at 495 nm, emission at 580 nm, annealing at 5 $^{\circ}$ C / min (black line), 1 $^{\circ}$ C / min (blue line) and 0.5 $^{\circ}$ C / min (red line), using a 1 cm quartz cell, 500 PMT voltage.

Steady-state fluorescence analysis of **1F** with complementary strands

10

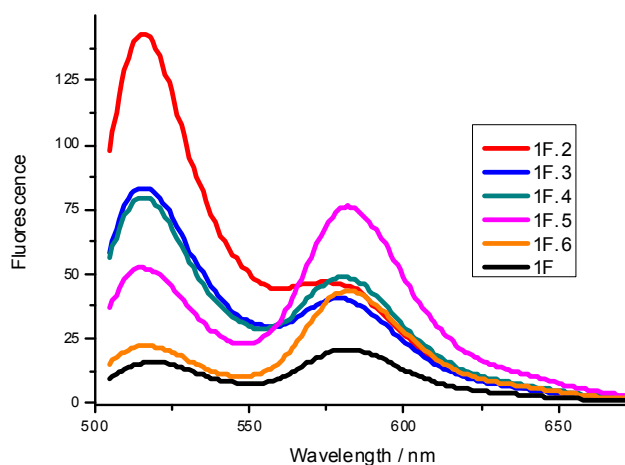


Figure S12. Steady-state fluorescence analysis of **1F** emission combinations, excitation at 495 nm, at 1 μ M in 0.1 M sodium phosphate buffer, using a 1 cm quartz cell, 500 PMT voltage. An additional reference spectrum of each sample at an excitation wavelength of 557 nm was used for the quantification of FRET efficiencies.

15

FRET simulations

The theoretical predictions of FRET were performed using a custom build MATLAB based program described elsewhere.^[4] The program simulates FRET based on an all-atom three-dimensional geometrical model of the nucleic acid constructed using individual base-pairs as building blocks and six standardized base-pair step parameters to describe each dinucleotide step in the structure (shift, slide, rise, tilt, roll and twist).^[5-9] To reconstruct the structures of the adjustable strap we used the base-pair step parameters for regular B-DNA derived from the calf thymus fiber models of Arnott and coworkers^[10,11] as implemented in w3DNA.^[12] For the calculation of FRET we defined the base-pair coordinate frame of each of the fluorescently modified bases and implemented these in the simulation software and the geometrical model building scheme (see below). The Cartesian coordinates of both the center and direction of the transition dipole moment vectors were

equally specified within these base-pair coordinate frames allowing the calculation of the exact donor-acceptor distances of the probes positioned in the geometrical DNA models built by the program.

Modelling the flexibly linked FAM/TAMRA probes

The definition of the local base-pair coordinate frame of the FAM/TAMRA probes attached to thymine using a hexyl linker is shown in Figure S13a and the corresponding Cartesian coordinates of transition dipole vectors are provided in Table S2. The center of the transition dipole was set in the center of the tricyclic ring and its direction pointing parallel to the long axis of the tricyclic framework. Since the hexyl linker provides diffusional mobility of the tethered probes relative to the DNA, the FAM/TAMRA dyes were positioned in their mean positions relative to the B-DNA helix as determined for the structurally similar Alexa 488 fluorophore by Sindbert *et al.* using MD simulations.^[13] In this respect, the mean position is not necessarily the most probable but it is the average of all the occupiable states and was shown by Sindbert *et al.* to be a good representation of the dye position in the calculation of FRET.^[13] Using this constraint for relative dipole position, the geometry of the linker and fluorophore were optimized using a force field for visual inspection only. The simulated geometries of all samples are show in Figure S14.

It is noted that Sindbert *et al.* found that the accessible volume of the dye attached to double-stranded DNA through the hexyl linker follows the helical twist of the groove.^[13] The average dye position thus has a z-displacement along the helix axis and as a result the mean pair distance for a given bp separation depends on whether the fluorophores are positioned 5'-3' or 3'-5' relative to one another. All calculated distances are shown in Table S3.

Modelling the rigidly linked porphyrin probes

The local base-pair coordinate frame and transition dipole coordinates of the porphyrin-modified bases are shown in Figure S13b and Table S2. Since the acetylenic linker provides a rigid attachment of the probe to the base we implemented the static, AM1 optimized geometries of the porphyrin modified thymine bases. The center of the transition dipole moment was set to be in the center of the porphyrin ring.

Table S2. Cartesian coordinates of dipole centers and directions of FAM/TAMRA attached to thymine using a hexyl linker and Zn/2H-porphyrin attached to thymine through an acetylenic linker within their local base-pair coordinate frames.

	x	y	z
<i>FAM/TAMRA:</i>			
Dipole center	0.86	12.69	5.06
Dipole end	0.33	13.26	5.68
<i>Porphyrin:</i>			
Dipole center	11.94	8.37	0
Dipole end	12.87	8.75	0

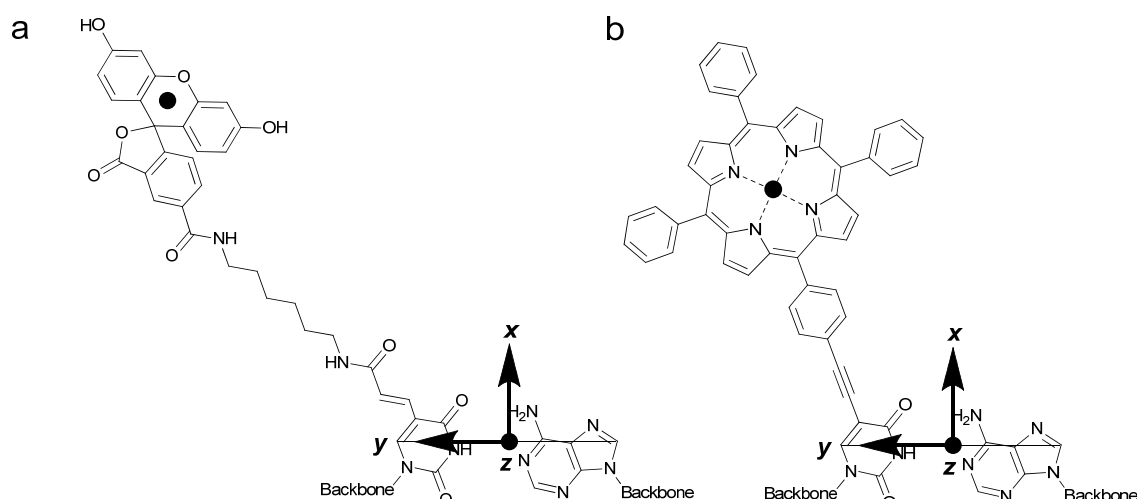


Figure S13. Definitions of local base-pair coordinate frames of the modelled dyes attached to thymine (in the Figure dyes are positioned in strand I). The origin of the coordinate frame is the mid-point of the line connecting the C8 of adenine and C6 for thymine. The *y*-axis is parallel to the C8-C6 line pointing from strand II to strand I. The *x*-axis points into the major groove while the *z*-axis completes a right-handed set.^[5,9] The dipole centres are marked as black dots, and the transition dipole moments. a) FAM/TAMRA molecular framework. b) Zn/2H-porphyrin molecular framework.

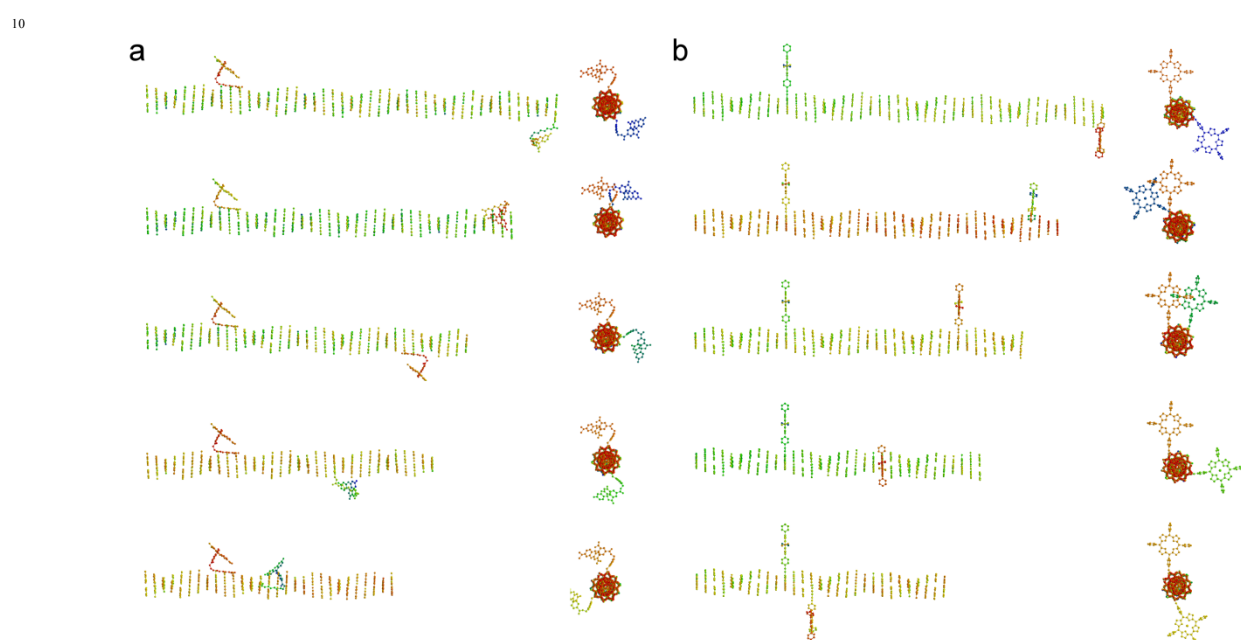


Figure S14. Side-views of simulated (ideal) three-dimensional geometries used for the theoretical predictions of FRET in the DNA switch going from sample 1.2 (top) to 1.6 (bottom). Only the spatial arrangement of the nucleobases is shown. A) FAM/TAMRA pair. B) Zn/2H-porphyrin pair. Note that Figure b shows the predicted structures of an ideally functioning switch functionalized with porphyrins, being different from what is observed experimentally (Figure S15).

Table S3. Theoretical mean-pair distances, R_{mp} ,^[13] of donor-acceptor pairs in the five states of an ideal DNA switch. Samples 1F.2, 1F.3, 1F.4, 1F.5, and 1F.6 denote the FAM/TAMRA system, while 1P.2, 1P.3, 1P.4, 1P.5, and 1P.6 denote the Zn/2H porphyrin system.

Sample	$R_{\text{mp}} / \text{\AA}$	Sample	$R_{\text{mp}} / \text{\AA}$
1F.2	117	1P.2	118
1F.3	103	1P.3	92.5
1F.4	78.9	1P.4	65.5
1F.5	54.3	1P.5	44.7
1F.6	27.3	1P.6	31.9

5

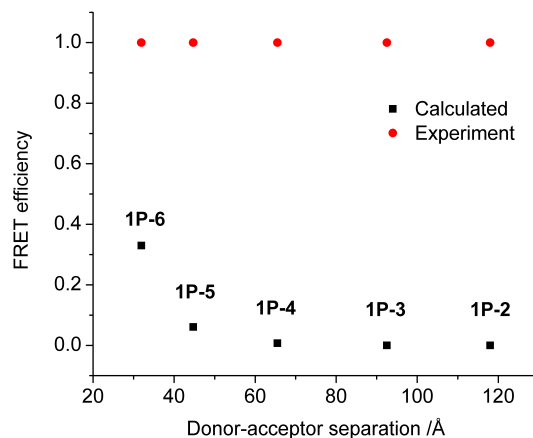


Figure S15. Measured and predicted FRET efficiencies of the DNA switch functionalized with porphyrins.
Predicted FRET efficiencies were calculated using the distances shown in Table S3 with $R_0 = 28.4 \text{ \AA}$.

10

Switching experiments with the 1F system

15

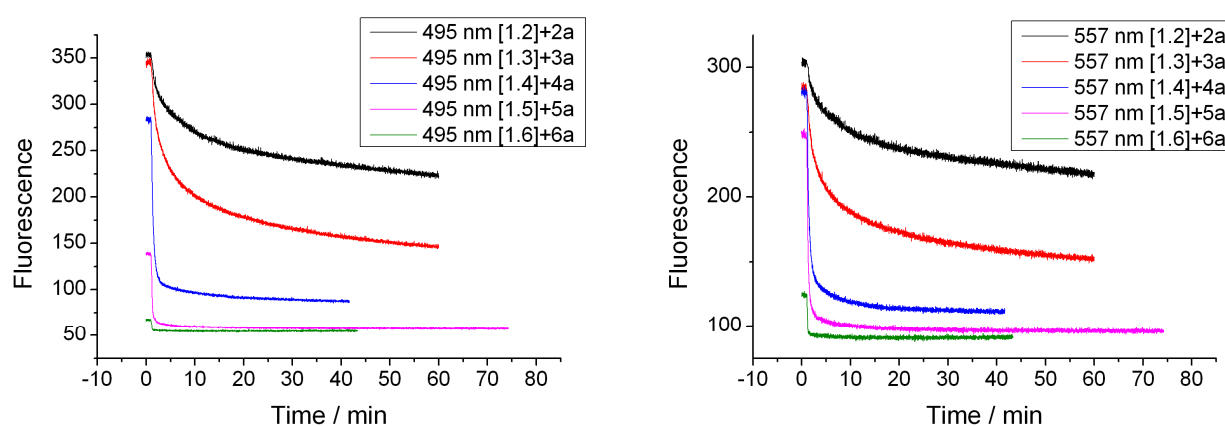


Figure S16. Release of the stabilising DNA strands (**2 – 6**) by addition of the complementary strands (**2a – 6a**; strand sequences see Table S1), monitoring the donor emission at 510 nm when exciting at 495 nm (left) and the acceptor emission at 580 nm when exciting at 557 nm (right). **1** at 0.5 μM , stabilising strands and release strands added in 1.1 molar excess.

20

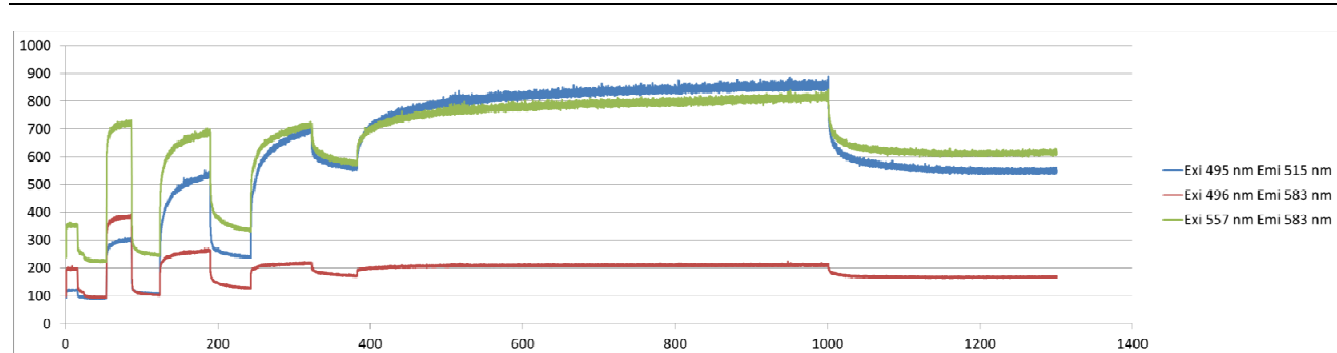


Figure S17. Switching of the **1F** system. Addition of DNA strands: see Table S4.

Table S4. Addition of stabilising and switching strands

Time (min)	Strand Added
0 to 16	1
1 to 16	6
16 to 54	6a / 2
54 to 86	2a / 6
86 to 123	6a / 3
123 to 189	3a / 6
189 to 243	6a / 4
243 to 323	4a / 6
323 to 377	6a / 5
377 to 1000	5a / 6
1000 to 1300	6a / 5

References:

1. L. A. Fendt, I. Bouamaied, S. Thöni, N. Amiot and E. Stulz, *J. Am. Chem. Soc.*, 2007, 129, 15319-15329.
2. A. Brewer, G. Siligardi, C. Neylon and E. Stulz, *Org. Biomol. Chem.*, 2011, 9, 777-782.
3. A. Mammana, T. Asakawa, K. Bitsch-Jensen, A. Wolfe, S. Chaturantabut, Y. Otani, X. X. Li, Z. M. Li, K. Nakanishi, M. Balaz, G. A. Ellestad and N. Berova, *Bioorg. Med. Chem.*, 2008, 16, 6544-6551.
4. S. Preus, K. Kilså, F. A. Miannay, B. Albinsson and L. M. Wilhelmsson, *Nucl. Acids Res.* (2012) doi: 10.1093/nar/gks856.
5. M. A. El Hassan and C. R. Calladine, *J Mol Biol*, 1995, 251, 648-664.
6. X. J. Lu, M. A. El Hassan and C. A. Hunter, *J Mol Biol*, 1997, 273, 681-691.
7. X. J. Lu, M. A. El Hassan and C. A. Hunter, *J Mol Biol*, 1997, 273, 668-680.
8. X. J. Lu and W. K. Olson, *Nucleic Acids Res*, 2003, 31, 5108-5121.
9. W. K. Olson, M. Bansal, S. K. Burley, R. E. Dickerson, M. Gerstein, S. C. Harvey, U. Heinemann, X. J. Lu, S. Neidle, Z. Shakded, H. Sklenar, M. Suzuki, C. S. Tung, E. Westhof, C. Wolberger and H. M. Berman, *J Mol Biol*, 2001, 313, 229-237.
10. S. Arnott and D. W. Hukins, *J Mol Biol*, 1973, 81, 93-105.
11. S. Arnott and D. W. L. Hukins, *Biochem Biophys Res Co*, 1972, 47, 1504-&.
12. G. Zheng, X. J. Lu and W. K. Olson, *Nucleic Acids Res*, 2009, 37, W240-246.
13. S. Sindbert, S. Kalinin, H. Nguyen, A. Kienzler, L. Clima, W. Bannwarth, B. Appel, S. Muller and C. A. Seidel, *J Am Chem Soc*, 2011, 133, 2463-2480.